



# The effect of polar end of long-chain fluorocarbon oligomers in promoting the superamphiphobic property over multi-scale rough Al alloy surfaces



Zubayda S. Saifaldeen<sup>a,b</sup>, Khedir R. Khedir<sup>a,b,\*</sup>, Merve T. Camci<sup>c</sup>, Ahmet Ucar<sup>c</sup>, Sefik Suzer<sup>c</sup>, Tansel Karabacak<sup>a</sup>

<sup>a</sup> Department of Physics and Astronomy, University of Arkansas at Little Rock, Little Rock, AR 72204, United States

<sup>b</sup> Department of Physics, College of Sciences, University of Duhok, Duhok, Kurdistan Region, Iraq

<sup>c</sup> Department of Chemistry, Bilkent University, Ankara 06800, Turkey

## ARTICLE INFO

### Article history:

Received 27 December 2015

Received in revised form 18 March 2016

Accepted 8 April 2016

Available online 9 April 2016

### Keywords:

Aluminum alloy

Micro-nano structure

Superamphiphobic

Fluorocarbon oligomer

Polar end

Conformality

Chemical stability

## ABSTRACT

Rough structures with re-entrant property and their subsequent surface energy reduction with long-chain fluorocarbon oligomers are both critical in developing superamphiphobic (SAP, i.e. both super hydrophobic and superoleophobic) surfaces. However, morphology of the low-surface energy layer on a rough re-entrant substrate can strongly depend on the fluorocarbon oligomers used. In this study, the effect of polar end of different kinds of long-chain fluorocarbon oligomers in promoting a self-assembled monolayer with close packed molecules and robust adhesion on multi-scale rough Al alloy surfaces was investigated. Hierarchical Al alloy surfaces with microgrooves and nanogras structures were developed by a simple combination of one-directional mechanical sanding and post treatment in boiling de-ionized water (DIW). Three types of long-chain fluorocarbon oligomers of 1H, 1H, 2H, 2H-perfluorodecyltriethoxysilane (PFDTs), 1H, 1H, 2H, 2H-perfluorodecyltrichlorosilane (PFDCS), and perfluorooctanoic acid (PFOA) were chemically vaporized onto these rough Al alloy surfaces. The PFDCS exhibited the lowest surface free energy of less than 10 mN/m. The contact angle and sliding angle measurements for water, ethylene glycol, and peanut oil verified the SAP property of hierarchical rough Al alloy surfaces treated with alkylsilane oligomers (PFDTs, PFDCS). However, the hierarchical surfaces treated with fluorocarbon oligomer with polar acidic tail (PFOA) showed highly amphiphobic properties but could not reach the threshold for SAP. Chemical stability of the hierarchical Al alloy surfaces treated with the fluorocarbon oligomers was tested under the harsh conditions of ultra-sonication in acetone and annealing at high temperature after different treatment times. Contact angle measurements revealed the robustness of the alkylsilane oligomers and deterioration of the PFOA coating particularly for low surface tension liquids. The robust adhesion and close-packing of the alkylsilane molecules as well as their vertical orientation with exposure of more CF<sub>3</sub> groups instead of CF<sub>2</sub> groups due to the polar silane-based tail are believed to be the main reasons behind their improved chemical stability. The selection of fluorocarbon oligomer with proper polar tail which can promote a self-assembled monolayer with close-packed molecules could make it possible for utilizing shorter fluorocarbon oligomers, which is environmentally favorable, to develop high surface energy materials with SAP properties.

© 2016 Elsevier B.V. All rights reserved.

## 1. Introduction

The discovery of lotus leaf with superhydrophobic (SHP) property [1], exhibiting water contact angle (CA) of more than 150° and sliding angle of less than 10°, more than a decade ago has

inspired both academia and industry to developing bioinspired artificial surfaces possessing such property for a wide range of potential technological applications [2,3]. This property of the lotus leaf, which is also known as “lotus effect”, is due to its surface’s hierarchical roughness incorporating micro- and nano-scale structures covered with a relatively low surface energy waxy material. However, SHP surfaces may not be able to exhibit lotus effect toward organic liquids with low surface tension of less than about 40 mN m<sup>-1</sup> compared to the water’s high surface tension of 72 mN m<sup>-1</sup>. A surface with lotus effect toward organic liquids such

\* Corresponding author at: Department of Physics, College of Sciences, University of Duhok, Duhok, Kurdistan Region, Iraq.

E-mail addresses: [krkhedir@ualr.edu](mailto:krkhedir@ualr.edu), [khedir.ramazan@uod.ac](mailto:khedir.ramazan@uod.ac) (K.R. Khedir).

as oils is known as the superoleophobic (SOP) surface. Lotus leaf, in spite of its SHP property, fails to repel low surface tension organic liquids and therefore is not SOP [4,5]. For technological applications such as self-cleaning and anti-fouling, surfaces demonstrating both the SHP and SOP property, which is known superamphiphobic (SAP), are highly desired. More details about SAP surfaces and their potential applications can be found in the following review articles [6,7].

It has been experimentally shown that for a solid substrate to repel any specific liquid possessing surface tension  $\gamma$ , surface energy of the substrate of less than about  $\gamma/4$  is required [8]. The lowest known surface energy materials in the descending order are  $\text{CH} > \text{CH}_2 > \text{CHF} > \text{CF}_2 > \text{CF}_3$ . Theoretically, the lowest surface energy material has been reported so far is for a smooth surface homogeneously coated with the close packed  $-\text{CF}_3$  molecules with a surface energy of 6 mN/m [9,10]. In order to impart SAP property to solid surfaces, an optimal surface roughness with re-entrant property followed by its coating with ultra-low surface energy materials such as long-chain fluorocarbon oligomers is required [6,7,11–16]. Low surface tension organic liquids such as oils with surface tension of less than 40 mN/m can still easily penetrate all the above mentioned low surface energy materials and homogeneously wet the surface. In order to avoid this, in addition to the ultra-low surface energy of a long-chain fluorocarbon oligomer, its molecules also need to densely coat the underlying re-entrant substrate. Such a close packing can prevent the oils from penetrating down to the high surface energy substrate [9] while re-entrant topography can stimulate the lotus effect. Fluorocarbon groups ( $\text{CF}_2$ ,  $\text{CF}_3$ ), in addition to their non-polarity, promotes the lowest non-polar dispersive interaction.

In the past, various techniques and materials have been used to engineer re-entrant rough structures in the shape of overhang structures [5,17], hierarchical micro- and nano-scale structures [11,16,18–20], nanoparticles [4,21,22], and interconnected fibers with knots [5,23]. It has been experimentally proven that the surface chemistry modification of rough surfaces with re-entrant structures with a long-chain fluorocarbon is crucial in facilitating SAP property, [11,13,16,24]. Zhao et al. [24] showed that textured silicon surface with a re-entrant property maintained CAs of more than  $150^\circ$  for low surface tension organic liquid of hexadecane only after the structures were coated with the long-chain fluorocarbon oligomers of  $\text{C}_8\text{H}_4\text{Cl}_3\text{F}_{13}\text{Si}$  (FOTS). However, the same textured surfaces after being coated with PTFE and the long-chain  $\text{C}_{18}$  hydrocarbon exhibited hexadecane CAs of  $121^\circ$  and  $0^\circ$ , respectively. Meng et al. [13] reported SAP zinc plates showed water and oil CAs of around  $158^\circ$  and  $155^\circ$ , respectively, after immersion in the long-chain fluorocarbon of nonadecafluorodecanoic acid ( $\text{C}_{10}\text{HF}_{19}\text{O}_2$ ). Meanwhile, in the same study, it was also shown that the Zn plates treated with pentadecafluorodecanoic acid ( $\text{C}_8\text{HF}_{15}\text{O}_2$ ) also showed SAP properties after changing the reaction conditions that led to the formation of rough structures with re-entrant property (Supporting information Fig. S6 of their article).

From the above mentioned studies one can conclude that for high surface energy rough structures with re-entrant property need to be treated with a long-chain fluorocarbon oligomer of carbon number  $n_C \geq 8$  and fluorine number  $n_F \geq 15$  in order to achieve SAP property. Meanwhile, for a rough re-entrant polymeric film that is made of a fluorocarbon material, SAP property can be obtained by using a short non-polar fluorinated tail. Bellanger et al. [11] reported SAP surfaces by electrodeposition of fluorinated 3,4-ethylenedioxy pyrrole (EDOP) with a short fluorine tail of F-hexyl with water and hexadecane, which showed CAs of higher than  $157^\circ$  and  $152^\circ$ , respectively. However, films prepared by the electrodeposition of EDOP(F-octyl) failed to show SOP property in spite of its longer fluorocarbon length, mainly due to the absence of re-entrant property.

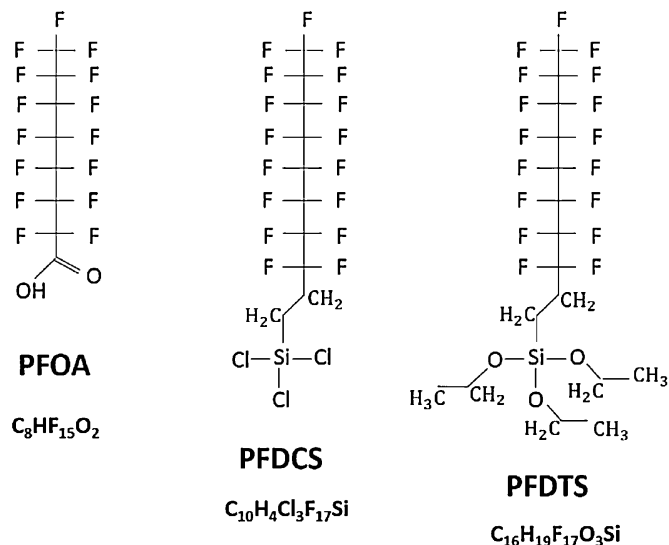


**Fig. 1.** A schematic representation of long-chain fluorocarbon oligomers of 1H, 1H, 2H, 2H-perfluorodecyltriethoxysilane (PFDTs), 1H, 1H, 2H, 2H-perfluorodecyltrichlorosilane (PFDCS), and perfluorooctanoic acid (PFOA).

Long-chain fluorocarbon oligomers possess both nonpolar (hydrophobic) and polar (hydrophilic) tails. The polar tail which is linked to the substrate can be either silane-based or acid-based groups. The hydrophobic tail with fluorocarbon molecules coming out of the surface is responsible for repelling the liquids. In previous studies on the impact of surface chemistry in developing SAP surfaces, most of the attention has been given to the structure of non-polar tail (fluorocarbon end) such as the effect of chain length on repelling low surface tension organic liquids. However, the role of polar tail in promoting a robust adhesion to the substrate as well as close-packing of the fluorocarbon molecules with vertical orientation is also crucial. In addition, the effect of multi-scale rough structures on the orientation of the fluorocarbon molecules has not been addressed yet. In this work, we investigated the wetting properties of hierarchically rough Al alloy substrates after being coated with two different alkylsilane oligomers 1H, 1H, 2H, 2H-perfluorodecyltriethoxysilane (PFDTs) and 1H, 1H, 2H, 2H-perfluorodecyltrichlorosilane (PFDCS) as well as with an acidic fluorocarbon oligomer perfluorooctanoic acid (PFOA). All these oligomers possessed non-polar tails of  $n_C \geq 8$ , which helped distinguishing the effect of polar tail on wetting properties (Fig. 1). Contact angle and sliding angle response of the samples was analyzed by using three different surface tension probe liquids of water, ethylene glycol, and peanut oil.

## 2. Materials and method

### 2.1. Developing multi-scale rough Al alloy surfaces

Multi-scale rough aluminum alloy surfaces were produced by first cutting an Al alloy sheet into  $2 \times 3$  cm pieces. Then, the substrates were cleaned for removal of contaminations and native oxide layer by wet-mechanical polishing with two different ultra-fine sandpapers of 2500 and 3000 grits. This was followed by ultra-sonication in acetone for 5 min and finally rinsing with DIW. The nanoscale rough Al alloy surface was developed by the immersion of the pre-cleaned flat substrate in boiling DIW for one minute. The microscale rough Al alloy with grove-like structures was produced by one-directionally sanding of the pre-cleaned Al alloy substrates using silicon carbide sandpaper of 60 grit with an associated particle diameter of  $\sim 500 \mu\text{m}$ . The hierarchical micro-nano-scale Al alloy surface was produced by simply immersing the

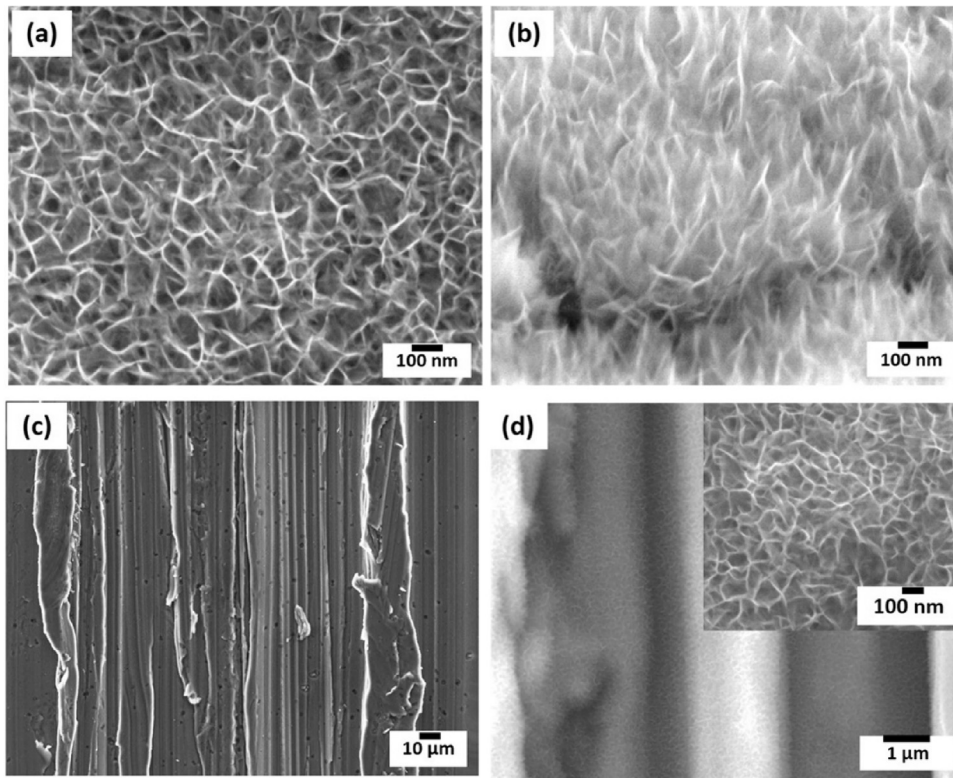


**Fig. 2.** SEM images of rough Al alloy surfaces of (a) top-view nanograss, (b) tilted-view nanograss, (c) microgrooves, and (d) hierarchical microgrooves-nanograss structures.

microscale rough Al alloy in boiling DIW for one minute. Surface morphology of the flat and multi-scale rough Al alloy surfaces was characterized using scanning electron microscopy (SEM).

## 2.2. Surface chemistry modification

In order to reduce the surface energy of flat and rough Al alloy samples, three different types of long-chain fluorocarbon oligomers of PFDTS, PFDCS, and PFOA (Fig. 1) were chemically vaporized onto smooth and roughened Al alloy substrates. For this purpose, a precursor was prepared by mixing a fluorocarbon oligomer with hexane. The volume ratio of each oligomer to hexane was pre-optimized by using different ratios as well as using a magnetic stirrer to obtain a highly homogenous precursor. Prior to surface chemistry modification, samples were first placed inside an oven under a temperature of 90 °C for 2 h. Next, for the low surface energy self-assembled monolayer coating, samples and precursor solution containing the selected fluorocarbon oligomer were placed in a sealed container (without having any physical contact) inside an oven which was set to 90 °C under ambient pressure. Precursor molecules were evaporated and arrived at the substrate surface through random gas phase collision within the container. After remaining inside the oven for 5 h, chemically modified surfaces were removed and left overnight under ambient conditions for rest of the chemical bonding process to be completed. The same process was followed for all of the pristine flat and rough Al alloy surfaces to be chemically modified by each of the three fluorocarbon oligomers.

## 2.3. Wetting characterization

Wetting characterization of the prepared surfaces was carried out by using a contact angle (CA) measurement system (VCAOptima). 5  $\mu$ l liquid droplets of water, ethylene glycol, and peanut oil were gently dispensed over the surfaces for their CA measurements.

Sliding angle (SA) was measured using a customized setup by dispensing 25  $\mu$ l liquid droplets. Tilt angle of the substrate at which the liquid droplet begins to slide is defined as the SA. For accuracy, CA and SA measurements were repeated three times and averaged for each sample.

## 2.4. Surface free energy

Surface free energy measurements for the three fluorocarbon oligomers coated on smooth Al alloy surfaces were carried out by the liquid probe method. Three conventional liquids water, ethylene glycol, and diiodomethane were utilized to determine the oligomers' total surface free energy as well as their energy components.

## 2.5. Surface chemistry and coverage characterization

In order to extract information about the surface chemistry and coverage of different types of oligomers on rough Al alloy substrates, X-ray Photoelectron Spectroscopy (XPS) was utilized using a Thermo Fisher K-alpha electron spectrometer with a monochromatic AlK $\alpha$  X-ray source that has an energy of 1486.6 eV. The homogeneity of the coatings was investigated using aerial two dimensional (2-D) spectral mapping, which was acquired by X-ray spot with a diameter of 100  $\mu$ m on consecutive points with intervals of 100  $\mu$ m, and recorded in the snapshot mode within F1s, C1s, O1s and Al2p regions.

## 2.6. Surface chemistry stability

Stability or robustness of the self-assembled monolayers of the fluorocarbon oligomers on hierarchically rough Al alloy surfaces was tested under harsh conditions. The pristine surfaces were ultrasonicated in acetone for various time periods of 5, 15, 30, and 60 min. Another set of samples were also annealed under high

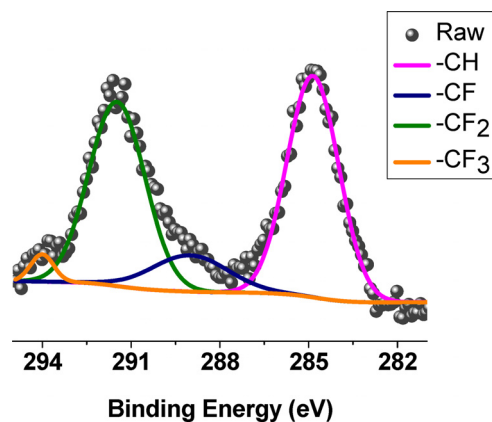


Fig. 3. A representative core level C1s XPS spectrum of the fluorocarbon oligomer coatings investigated in this study.

temperature of 200 °C for various time periods of 2, 4, 6, and 8 h in ambient pressure. After each treatment time of both ultrasonication in acetone and annealing process, CA measurements were carried out for water, ethylene glycol, and peanut oil. The same process was repeated for the entire hierarchical rough Al alloy surfaces, which were chemically modified with the three different types of fluorocarbon oligomers.

### 3. Results and discussion

#### 3.1. Surface morphology

Surface morphologies of the rough Al alloy surfaces captured by SEM are shown in Fig. 2. Fig. 2a and b exhibit the top and tilted-views of the nanoglass structures obtained by immersion of the polished (flat) Al alloy sheet in boiling DIW. The analysis of top view and tilted view SEM images showed that the nanostructures have the lateral size of around 10 nm and a vertical height of about 200 nm. Nanostructures also formed interlinked thin sheets resulting in a porous structure with an approximate pore diameter of ~100 nm. Microgrooves, shown in Fig. 2c, developed by one-directional mechanical sanding possess the anisotropic microgrooves with an average channel width of around 10 μm and overall roughness ( $R_a$ ) of  $3.3 \pm 0.2 \mu\text{m}$ .

Moreover, Fig. 2d shows a magnified SEM of hierarchically rough Al alloy surface that incorporates microgrooves covered by nanoglass structures. The image reveals the conformal coverage of microgrooves with nanoglass. Presence of nanoglass structures on the inner walls of microgrooves provides a re-entrant property to the surface's overall texture. In addition, the surface also possesses a higher degree of roughness compared to the individual cases of microgrooves and nanoglass surfaces [16].

#### 3.2. Fluorocarbons' surface chemistry

Fig. 3 shows a representative core level C1s spectrum of the fluorocarbon oligomer coatings investigated in this study after they were evaporated on rough Al substrates. The profiles involve four-different photoelectron peaks corresponding to -CH (284.85 eV), -CF (289.01 eV), -CF<sub>2</sub> (291.48 eV) and -CF<sub>3</sub> (294.01 eV) groups, which are consistent with the theoretical molecular structures of the oligomers illustrated in Fig. 1.

#### 3.3. Fluorocarbons' surface free energies

It is vital to determine the surface free energies of the fluorocarbon oligomers chemically vaporized onto the polished Al alloy

Table 1

Calculated values of surface free energy along with its polar and nonpolar components for the fluorocarbon oligomers of this study.

Fluorocarbon Oligomer	$\gamma_s^d$ (mN/m)	$\gamma_s^+$ (mN/m)	$\gamma_s^-$ (mN/m)	$\gamma_s$ (mN/m)
PFDTS	7.96	0.27	1.06	10.27
PFDCS	6.36	0.13	1.23	8.7
PFOA	7.62	0.03	1.16	9.81

surfaces. Surface free energy components of low surface energy solids ( $\gamma_s$ ) and liquids ( $\gamma_l$ ) are resolved into both non-polar (Lifshitz-van der Waals) dispersive energy ( $\gamma^d$ ) and polar energy ( $\gamma^\pm$ ) with both components of Lewis acid ( $\gamma^+$ ) and Lewis base ( $\gamma^-$ ), according to the following formulas:

$$\gamma_s = \gamma_s^d + 2(\gamma_s^+ + \gamma_s^-)^{1/2} \quad (1)$$

$$\gamma_l = \gamma_l^d + 2(\gamma_l^+ + \gamma_l^-)^{1/2} \quad (2)$$

The surface free energy components ( $\gamma_s^d$ ,  $\gamma_s^+$ ,  $\gamma_s^-$ ) of the fluorocarbon oligomers of this study were determined by using the measurements of  $\theta$  for water, ethylene glycol, and diiodomethane (zero-polar liquid), and contributing them in the Van Oss-Chaudhury-Good's equation:

$$\gamma_l(1 + \cos\theta) = 2(\gamma_l^d \gamma_s^d)^{1/2} + 2[(\gamma_s^+ \gamma_l^-)^{1/2} + (\gamma_l^+ \gamma_s^-)^{1/2}] \quad (3)$$

Measured CAs of the three probe liquids along with their surface tensions and associated polar and nonpolar components were substituted into Eq. (3) to determine the surface free energy components of each fluorocarbon oligomer. The  $\gamma_s$  of each fluorocarbon oligomer was determined by substituting their obtained surface free energy components into Eq. (1). The values of  $\gamma_s$  and  $\gamma_s^d$ ,  $\gamma_s^+$ ,  $\gamma_s^-$  for the three fluorocarbon oligomers are listed in Table 1. It can be noticed that the  $\gamma_s$  of the three fluorocarbon oligomers are in the range of 8–10 mN/m, which are in good agreement with the reported values of (9–11 mN/m) for fluorocarbon oligomers with  $-(C_n F_{2n+1})$  and  $n=8-10$  coated on gold substrate. Among the three fluorocarbon oligomers, PFDCS showed the lowest  $\gamma_s$  of 8.7 mN/m while PFDTS with the highest  $\gamma_s$  of 10.27 mN/m. In spite of its longest carbon chain length, PFDTS did not show the lowest surface energy after being vapor coated onto the surfaces of flat Al alloy. Furthermore, it can also be noticed that most of the three fluorocarbon oligomers'  $\gamma_s$  is contributed by their nonpolar components of  $\gamma^d$ , which is expected from a low surface energy oligomers. From the two polar components, values of Lewis base  $\gamma^-$  component are relatively much higher than values of Lewis acid  $\gamma^+$  component for all the fluorocarbon oligomers we studied.

CA values for the liquids with different surface tensions measured on the flat and rough Al alloy surfaces coated with the three different fluorocarbon oligomers are plotted in Fig. 4. The values of CA for water, ethylene glycol, and peanut oil decrease with the decrease in the liquid's surface tension for all the three fluorocarbon oligomers (PFDTS, PFDCS, and PFOA). This trend of CAs versus the liquid's surface tension is consistent with the Young's model ( $\theta = \cos^{-1}[\gamma_s - \gamma_{sl}/\gamma_l]$ ), where  $\gamma_{sl}$  represents the surface energy at the solid-liquid interface. The equation shows that the spreading tendency of a liquid droplet while being deposited on a solid surface increases with the decrease of liquid's surface tension and therefore exhibits a lower CA.

Meanwhile, as shown in Fig. 4, fluorocarbon oligomers we studied demonstrated different behavior in repelling liquids depending on both the surface roughness and surface chemistry of the substrate. For flat Al alloy samples (Fig. 4a), the surface coated with PFDCS showed highest CAs of 125, 115, and 89° for water, ethylene glycol, and peanut oil, respectively. These CAs are about 5° and 14° higher for water, 8° and 13° higher for ethylene glycol, and 5° and 18° higher for peanut oil compared to the CAs observed on the flat

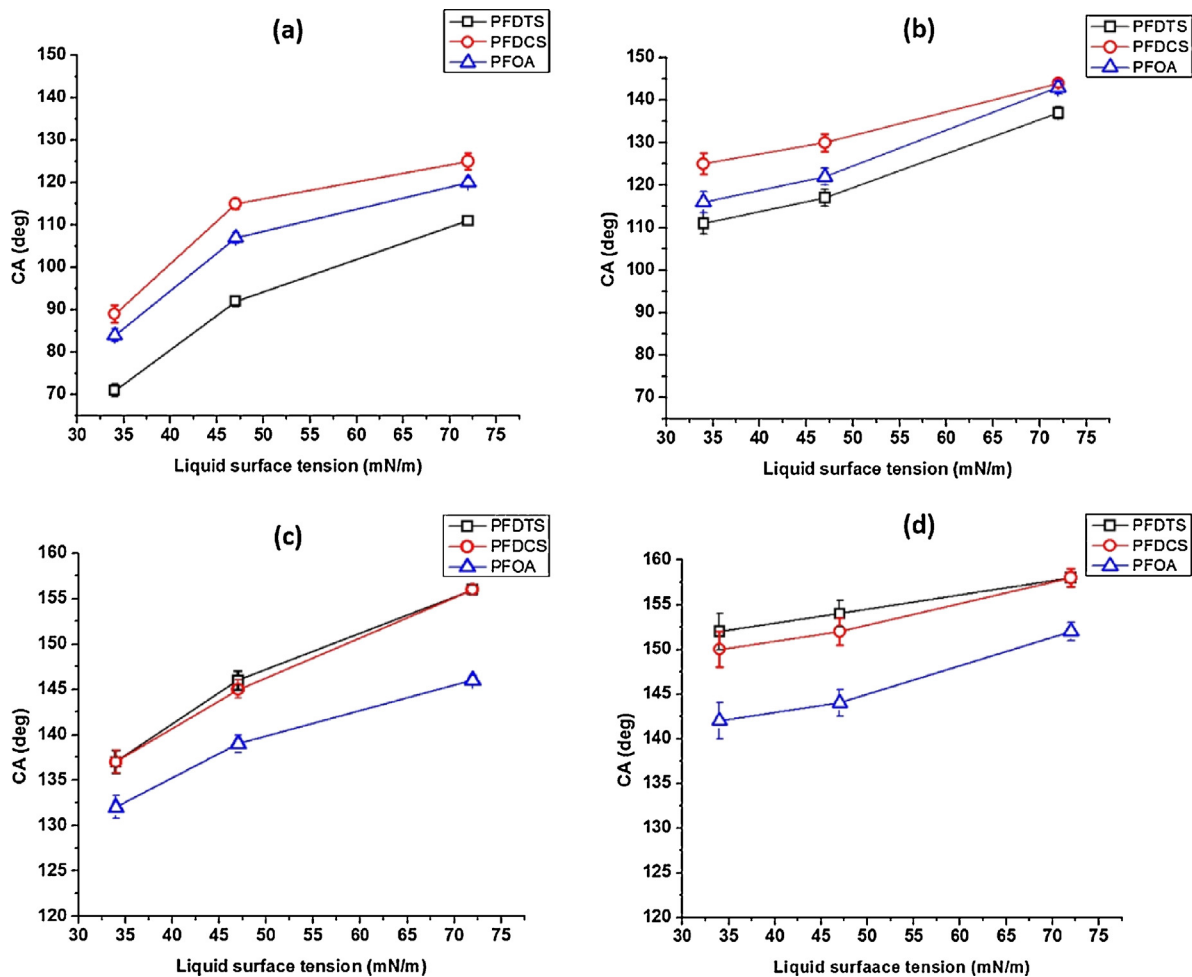


**Fig. 4.** Contact angle (CA) profiles for the water, ethylene glycol, and peanut oil on the surfaces of (a) flat, (b) microgrooves, (c) nanograss, and (d) hierarchical microgrooves-nanograss Al alloy substrates that were coated with the three different fluorocarbon materials (PFDTS, PFDCS, PFOA).

surfaces coated with PFOA and PFDTS, respectively. This is in good agreement with the calculated values of the surface free energies of the fluorocarbon oligomers listed in Table 1. In the case of Al alloy surface with microgrooves (Fig. 4b), PFDCS and PFOA still show higher CAs of around  $5^\circ$  for all the three liquids compared to the surface coated with the PFDTS, in spite of the PFDTS' longer carbon chain.

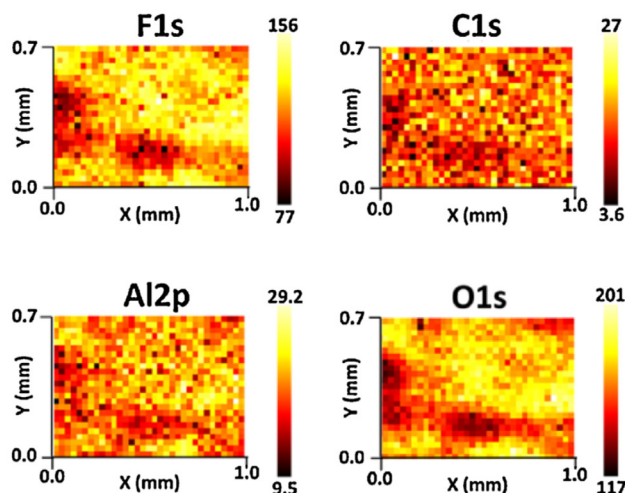
However, for nanograss and hierarchical Al alloy samples (Fig. 4c and d), the surfaces coated with alkylsilane oligomers PFDTS and PFDCS showed significantly higher CAs compared to the surfaces coated with PFOA. In general, nanograss and hierarchical surfaces coated with PFDTS exhibited relatively greater CAs compared to PFDCS, which had higher CAs on flat and microgroove Al alloy surfaces. For nanograss structures (Fig. 4c), the surfaces coated with the two alkylsilanes showed relatively comparable CA values for the three liquids, which were higher more than  $10^\circ$  for water and  $5^\circ$  for peanut oil compared to those with PFOA. In the case of hierarchical Al alloy samples (Fig. 4d), the surfaces coated with PFDTS and PFDCS showed similar CAs of around  $158^\circ$  for water and about  $154^\circ$  and  $152^\circ$  for ethylene glycol and peanut oil, which were about  $10^\circ$  higher compared to the CAs of same surfaces coated with PFOA.

Comparing the wetting properties of flat and microgrooved Al alloy surfaces coated with the fluorocarbon oligomers of this study, it is observed that PFDTS resulted in the lowest CAs in spite of its longest carbon chain-length of 16 compared to 10 and 8 for PFDCS and PFOA, respectively. On the other hand, these flat and microscale rough Al alloy surfaces presented highest CAs when coated with the

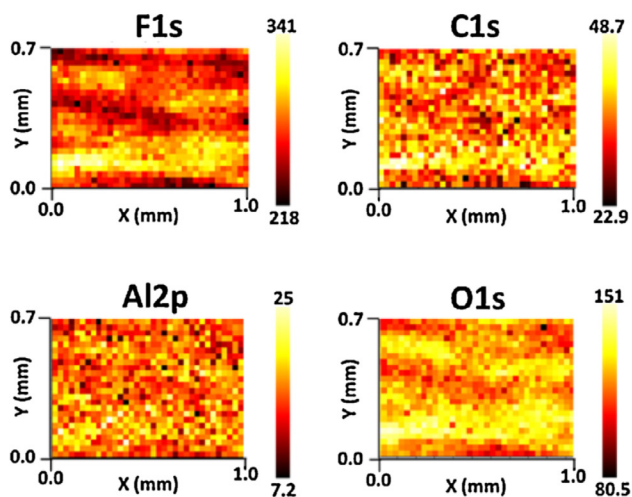
PFDCS, although it did not have the longest carbon chain-length, but the same fluorocarbon chain-length (nonpolar tail) of PFDTS. This is believed to be due to that PFDCS's polar tail chlorosilane ( $\text{SiCl}_3$ ) might have provided a more close-packed self-assembled monolayer with vertical orientation of its molecules to the substrate, which results in the lowest surface free energy among the fluorocarbons we investigated. In addition, PFOA showed higher wetting repellency compared to PFDTS in spite of PFOA's significantly shorter carbon chain and one less  $\text{CF}_2$  group.

However, in the case of Al alloy samples with nanograss and hierarchical microgrooves-nanograss structures, the two alkylsilanes of PFDTS and PFDCS showed significantly higher CAs for the entire range of the liquids' surface tensions. This might be due to the potential difference in surface coverage of the fluorocarbon oligomers used in this study. Because we used an evaporation method to coat the samples with these oligomers, the molecular weight of a given fluorocarbon oligomer can affect the mean-free-path of its molecules in the vapor phase, which can in turn influence the flux distribution on the substrate. The molecules of a more uniform random flux formed by small mean-free-paths can coat the rough surfaces more uniformly (i.e. conformally) in a process similar to that of chemical vapor deposition; while, on the other hand, it might suffer from non-uniform coverage due to a shadowing effect when the flux is more directional [25]. Fig. 5 shows the 2-D XPS area profiles of PFOA, PFDTS and PFDCS coated hierarchically rough Al samples. These area profiles consist of two axes (x and y)

## PFOA



## PFDTs



## PFDCS

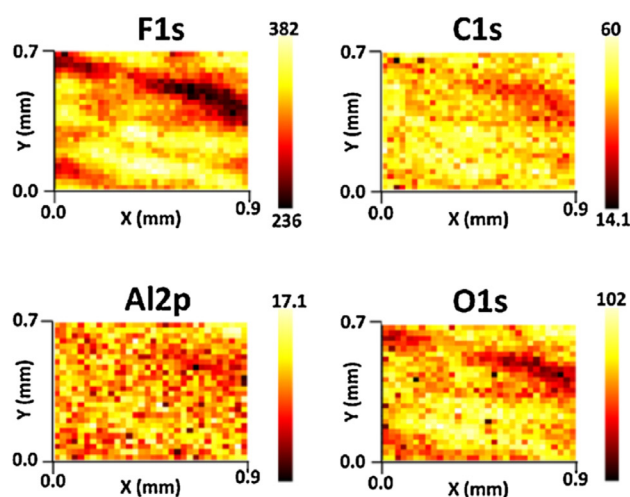


Fig. 5. 2-D XPS area profiles of PFOA, PFDTs, and PFDCS coated on hierarchically rough Al substrates.

that show the positions in millimeter-scale and an additional color bar corresponding to the peak intensity, computed as the area. Since all of the oligomers contain  $-\text{CF}_2$  groups in their structure, the area profiles obtained by analysis of the C1s peak observed around 291.5 eV and the F1s peak should be correlated in the intensity manner. Moreover, the area profiles recorded from Al2p and O1s regions which reveal information about the morphology of underlying Al alloy substrates (i.e. brighter color for higher surface points) are also expected to be correlated with each other. In addition to these expected correspondences between C1s and F1s peaks plus Al2p and O1s peaks, the signal intensity coming from fluorocarbon molecules was observed to be matched to that of Al signal intensity coming from the substrate in these mapping profiles, even though the signal intensity arising from the underlying substrate should be observed to decrease upon the overlayer deposition on top. In other words, the intensity profiles of all of the oligomers closely followed the topography of the substrate. These results indicate that all of the oligomers investigated in this study conformally coated the rough Al substrates, which eliminates

the hypothesis of different surface coverage due to the possible difference in their flux distribution during evaporation.

Another and more likely origin of higher CAs observed for PFDTs and PFDCS on nanoglass and hierarchical substrates is that higher oxidized surface (alumina) area of these samples can provide more favorable bonding sites towards alkylsilanes due to the presence of higher rate of hydroxyl ( $-\text{OH}$ ) groups compared to flat and microgrooved Al alloy surfaces with lower rate of native  $-\text{OH}$  groups. In addition, the nanoscale roughness of the nanoglass structures could have also helped in facilitating more close-packing of alkylsilanes molecules and consequent vertical orientation of their molecules. Sizes of the oligomer molecules of this study are in the nanoscale range of around 5–10 nm [26], which can cause orientation of the molecule be affected by the nanoscale roughness of the alumina nanoglass structures having lateral sizes of about 10–15 nm. In addition, alkylsilane oligomers PFDTs and PFDCS both exhibited similar CA values in spite of the difference in their carbon chain length. All these indicate to the significant role of the polar tail of fluorocarbon oligomer in terms of providing close-packing mono-

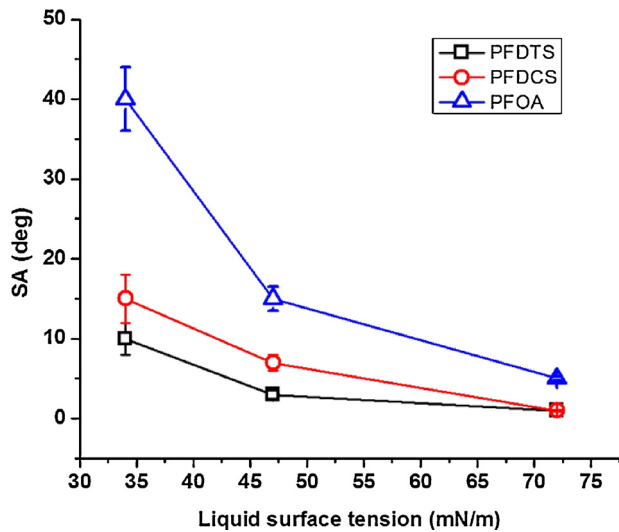


Fig. 6. Sliding angle (SA) profiles of water, ethylene glycol, and peanut oil on the hierarchical microgrooves-nanograss structures coated with different long-chain fluorocarbons (PFDTs, PFDCS, PFOA).

layer and the way that its molecules are oriented. Consequently, the robustness and surface free energy of the substrates coated with the fluorocarbon oligomers can be associated with all these factors.

Kinetics of the liquid droplet on a tilted substrate could provide a better insight into the homogeneity and close packing of the fluorocarbon oligomers on Al alloy surfaces. For a liquid droplet to slide over a rough surface coated with a fluorocarbon oligomer, it has to overcome the adhesion forces at the liquid-solid interface as a result of surface's contact angle hysteresis (CAH). The CAH arises from the existence of various localized microscopic CAs at the contact area due to the physical (roughness) and chemical heterogeneities of the surface [17,27–29]. A monolayer of fluorocarbon oligomer enriched with more close-packed and vertically oriented molecules can significantly reduce the surface's CAH. In the case of CAH due to the surface roughness, a surface texture with optimal roughness and re-entrant property can facilitate partial wetting of the surface with unstable liquid-solid contact line. For a liquid droplet to roll off over the surface by tilting it, the droplet has to overcome the surface's CAH. Lower CAH means smaller SA for the liquid droplet to roll off. Fig. 6 shows the values of SAs of the three liquids with various surface tensions over the hierarchical Al alloy surfaces coated with the three different fluorocarbon oligomers. The surface coated with PFDTs exhibited the lowest SAs of less than  $10^\circ$  for all the three liquids and the only surface to be recognized as the SAP surface with lotus effect property. In the case of surface coated with PFDCS, it also showed low SAs of less than  $10^\circ$ , but only for the high and moderate surface tension liquids of water and ethylene glycol, respectively. It showed significantly high SA of more than  $30^\circ$  for the low surface tension peanut oil. Meanwhile, the surface coated with PFOA showed the highest SAs compared to the surfaces coated with silane-based fluorocarbon oligomers of PFDTs and PFDCS. The surface demonstrated lotus effect property only for the case of high surface tension liquid of water. In the case of water, the surface covered with  $\text{CF}_2$  molecules can facilitate low adhesion and consequent low SA. However, low SAs of oils indicate dominant coverage of  $\text{CF}_3$  molecules on the solid surface. Accordingly, SA results reveal that hierarchical Al alloy surface coated with PFDTs has provided the best conformity and close-packing coating. However, there still might be a scenario where the fluorocarbon oligomer's molecules to be horizontally stacked on the surface without tightly adhering to the substrate through its nonpolar tail. Therefore, the robustness test of the coating may provide more details about the adhesion sta-

bility and close-packing of the fluorocarbon oligomers of this study. These results are in good agreement with the studies conducted by Hozumi and McCarthy [30,31], where they showed negligible CAH for smooth and nano-rough oxidized Al surfaces coated with long-chain fluorocarbon oligomers (PFDTs) for both water and *n*-hexane. The results were attributed to the monolayer oligomer coating by chemical vapor deposition and subsequent umbrella-like coverage of the surfaces with  $\text{CF}_3$  molecules.

### 3.4. Work of adhesion calculations

The quantification of the adhesion properties of the three fluorocarbon oligomers coated on the hierarchical rough Al alloy surfaces can be carried out by determining their associated work of adhesion. For a liquid droplet to slide over the solid surface, an applied force of equal or greater than the work of adhesion ( $W_{ad}$ ) at the solid-liquid interface is required. According to the Young-Dupre relation, the  $W_{ad}$  between a liquid droplet and a physically and chemically homogenous solid surface can be represented as:

$$W_{ad} = \gamma_{lv} (1 + \cos\theta) \quad (4)$$

where  $\gamma_{lv}$  represents the surface energy at the liquid-vapor interface. For a rough solid surface that is partially wetted by adopting the Cassie state or the metastable Cassie state of wetting, the droplet contact area is partially in contact with the solid surface. Therefore, according to the modified Young-Dupre relation for determining  $W_{ad}$  of rough surfaces [32,33]:

$$W_{ad} = \gamma_{lv} f (1 + \cos\theta) \quad (5)$$

Empirically, the surface's solid fraction in contact with the three different liquids can be determined using Cassie relation, in which  $f$  is the function of both associated apparent and intrinsic CAs.

$$f = \frac{1 + \cos\theta^*}{1 + \cos\theta} \quad (6)$$

And subsequently,

$$W_{ad} = \gamma_{lv} (1 + \cos\theta^*) \quad (7)$$

The values of both  $\theta$  and  $\theta^*$  represent the macroscopic picture of the interfacial interaction of wetting mechanism of only around the contact line, which represents a meeting line of the air-liquid-solid phases, without considering the interfacial interaction at the central contact area of the three phases of the solid-liquid interface. Thus, the above equation determines the solid fraction only on the premier of the contact area around the contact line (triple line). In a recent study by Bormashenko and his coworker [34], it was demonstrated that the liquid CA is only governed by the adjacent area around the triple line which is a narrow area around the premier of the contact area. Meanwhile, the adhesion of the droplet to the surface is governed by the entire interfacial contact area. Thus, more precise and comprehensive values of  $f$  can be determined by considering both static and kinetic wetting parameters represented by the CA and SA values, respectively. In addition, the solid surface's physical and chemical heterogeneities, which is quantified as CAH, cause increase in the adhesion. For a liquid droplet to slide at a specific surface tilting angle  $\alpha$  (SA) due to its weight of ( $\rho Vg$ ), the droplet must overcome all the energy barrier manifested as the  $W_{ad}$  at the entire contact area of the solid-liquid interface, as follows [32].

$$f = \frac{2(\rho Vg) \sin\alpha}{\pi w \gamma_{lv} (1 + \cos\theta)} \quad (8)$$

Here  $f$  is the function of the surface's wetting properties in the form of static ( $\theta$ ) and kinetics ( $\alpha$ ) parameters, in addition to the liquid's physical properties ( $\rho Vg/\gamma_{lv}$ ) and the width of the contact area ( $w$ ).

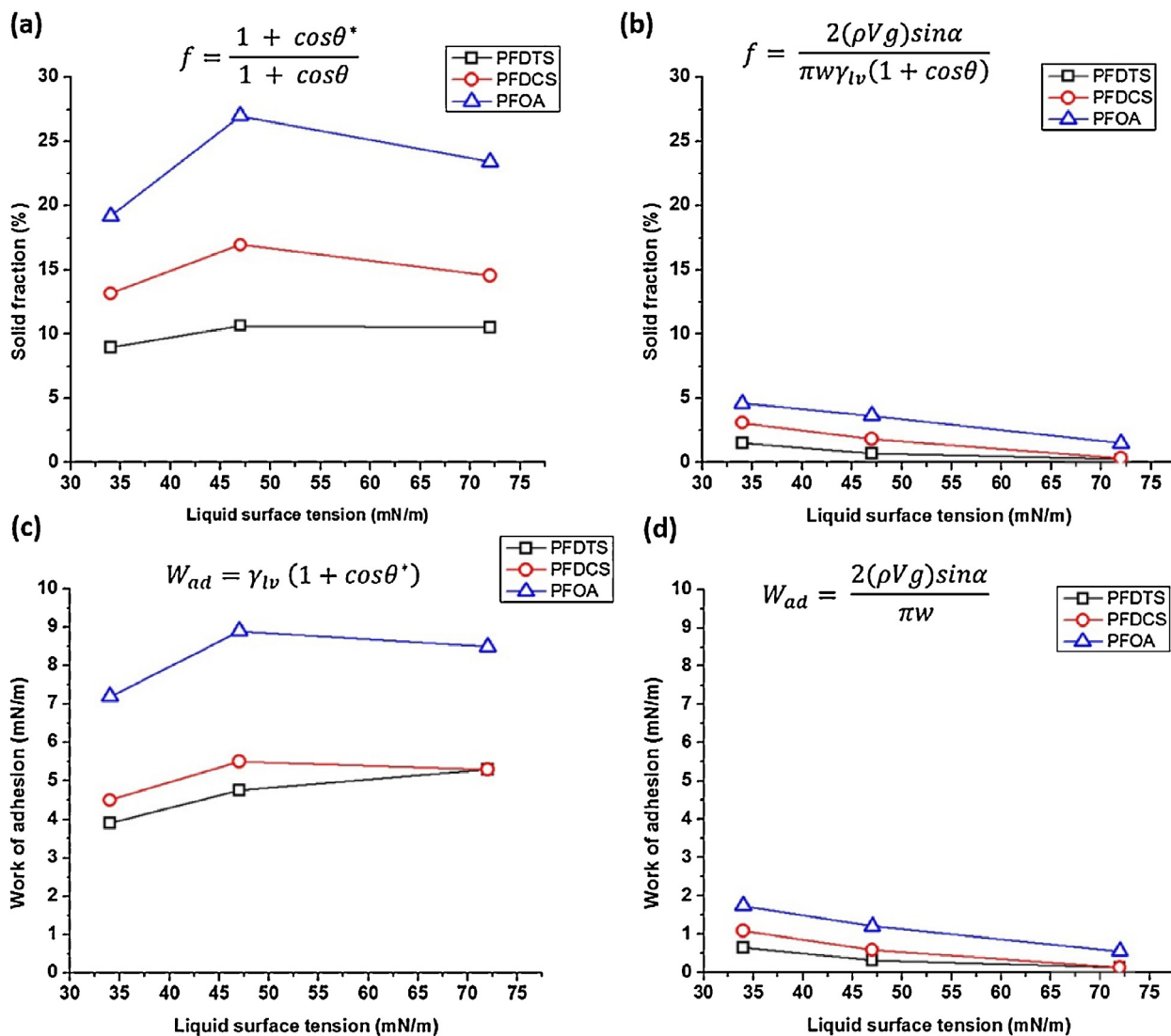


Fig. 7. The values of work of adhesion ( $W_{ad}$ ) and solid fraction percentages ( $f$ ) versus the liquids' surface tensions for the hierarchical Al alloy surfaces coated with fluorocarbon oligomers of PFDTs, PFDCS, and PFOA.

Substituting Eq. (5) into the Eq. (2),  $W_{ad}$  for a liquid droplet partially wetting the rough solid surface is given as:

$$W_{ad} = \frac{2(\rho V g) \sin\alpha}{\pi w} \quad (9)$$

Fig. 7 shows the calculated values of solid fractions and work of adhesions between the three liquid droplets and the hierarchical Al alloy surfaces coated with PFDTs, PFDCS, and PFOA. Using the macroscopic values of intrinsic CA ( $\theta$ ) and apparent CA ( $\theta^*$ ) and utilizing Cassie relation Eq. (3) to determine  $f$  (Fig. 7a), Eq. (4) resulted in corresponding  $W_{ad}$  values plotted in (Fig. 7c). The values of both  $f$  and  $W_{ad}$  increased with the decrease in their corresponding values of  $\theta^*$ , which is consistent with the fact that higher CAs is the indication of having smaller contact area and consequent lower adhesion. However, peanut oil droplet in spite of possessing the lowest CA and greatest SA values compared to both water and ethylene glycol showed the lowest  $f$  and consequent minimum  $W_{ad}$  for the all three different fluorocarbon oligomers. This is inconsistent with the general understanding that lower surface tension liquids tend to wet larger solid areas and leads to subsequent larger adhesion. Fig. 7b and d show the val-

ues of both  $f$  and  $W_{ad}$  after considering the kinetics of droplets motion in addition to macroscopic values of intrinsic CAs. Using Eqs. (5) and (6), the trends of the calculated values of both  $f$  and  $W_{ad}$  are consistent with the corresponding values of measured SAs (Fig. 6). Higher CAs and lower SAs is the manifestation of less  $f$  in contact with the liquid droplets and consequent lower  $W_{ad}$  to overcome.

The hierarchical surfaces coated with both PFDTs and PFDCS oligomers showed similar values of  $f$  and consequently similar  $W_{ad}$  values for water (Fig. 7b and d). For ethylene glycol and peanut oil, the surfaces coated with PFDTs exhibited lower  $f$  as well as  $W_{ad}$  compared to the surfaces coated with PFDCS. Meanwhile, the surfaces coated with PFOA oligomer showed significantly higher values for both  $f$  and  $W_{ad}$  compared to the surfaces coated with the two silane-based fluorocarbon oligomers (PFDTs and PFDCS). The results are consistent and follow a very similar trend of the observed values of the surfaces' SAs depicted in Fig. 6. These results indicate that the wetting analysis of solid surfaces cannot be comprehensive and precise without considering both static ( $\theta$ ,  $\theta^*$ ) and kinetic ( $\alpha$ ) properties of liquid droplets on the surface.

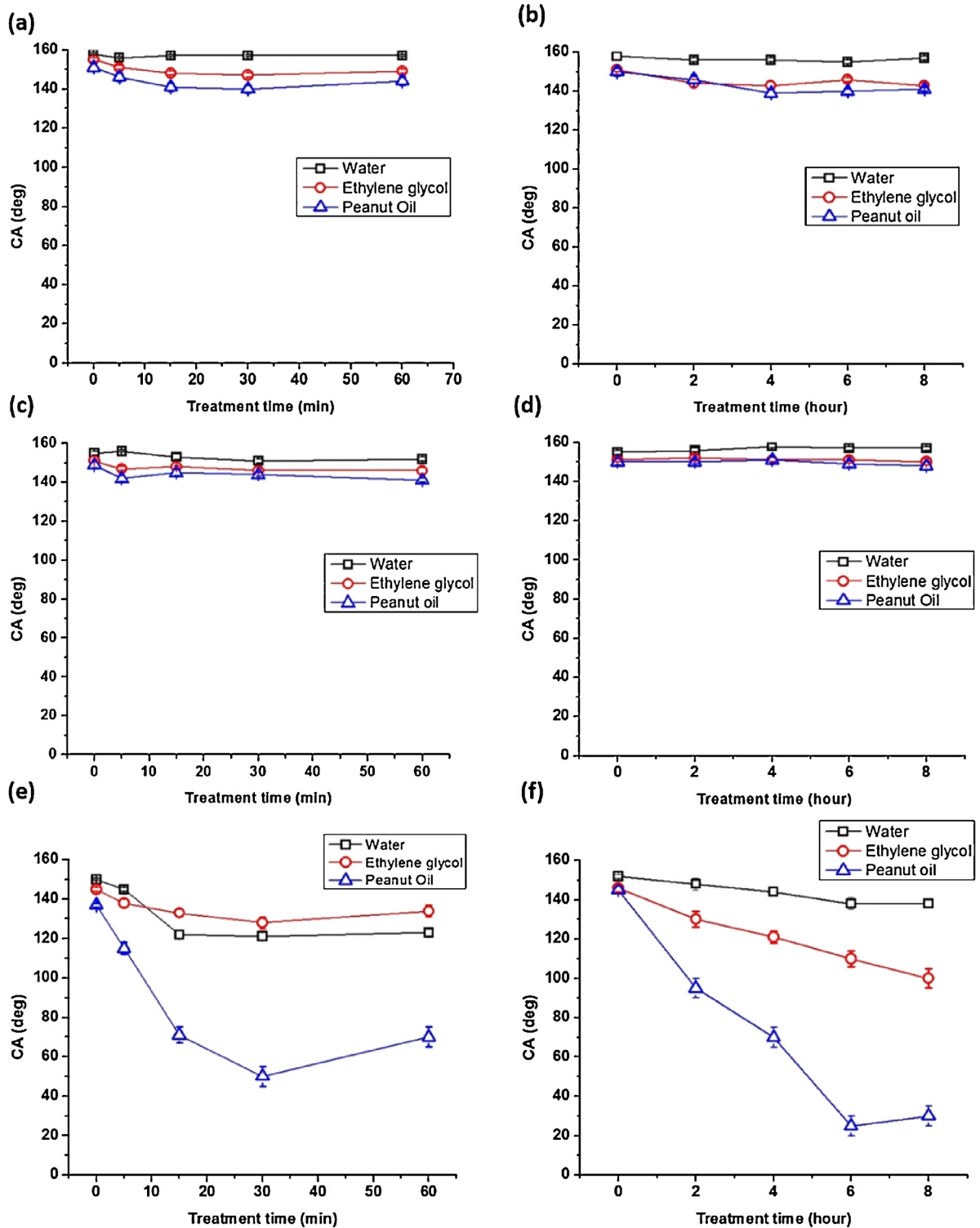


**Fig. 8.** CA values of water, ethylene glycol, peanut oil on the hierarchical Al alloy surfaces coated with PFDTs (a and b), PFDCS (c and d), and PFOA (e and f) after ultra-sonication of the surfaces in acetone for various time periods of 0, 5, 15, 30, and 60 min (a, c, e), and annealing at 200 °C for various time periods of 0, 2, 4, 6, and 8 h (b, d, f).

### 3.5. Surface chemistry stability

Robustness and chemical stability of the fluorocarbon oligomers after being vapor coated on the hierarchical microgrooves-nanogras Al alloy surfaces is of great importance in assessing their molecules' close-packing and robust adhesion to the substrate. A stable coating can be achieved by the strong covalent bonding of oligomer molecule through its polar tail to the surface, which also

facilitates a vertical orientation of the molecule. Fig. 8 shows the CA values of the hierarchical surfaces coated with PFDTs, PFDCS, and PFOA after their ultra-sonication in acetone and annealing as a function of time. For the surfaces coated with PFDTs, after ultra-sonication in acetone (Fig. 8a), the water CAs experienced almost no change even after 60 min of treatment. However, a maximum decrease of about 7–10° in the CAs of both ethylene glycol and peanut oil was observed. The annealing of the surfaces at ambient

conditions under 200 °C temperature (Fig. 8b) had a very similar effect on the values of the liquids' CAs. The water CAs kept unchanged even after 8 h of the treatment. After a slight decrease in the CA values of both ethylene glycol and peanut oil after 2 h, they got reduced of  $\sim 10^\circ$  after 8 h of annealing. For the surfaces coated with PFDCS, after ultrasonication in acetone, water CAs were stable for the whole treatment time (Fig. 8c). However, there was a slight decrease of less than  $8^\circ$  in the CA values of both ethylene glycol and peanut oil. Even after the annealing process of up to 8 h, almost no decrease in the CA values for any of the liquids was observed (Fig. 8d). This shows significant robustness of the PFDCS under high temperatures. On the other hand, for PFOA, ultra-sonication and annealing treatments caused significant reductions in CAs, which indicate substantial degradation of the coating. PFOA samples suffered from peanut oil CAs dropping by as much as  $70$  and  $120^\circ$ , after the 60 min ultrasonication and 8 h annealing treatments, respectively (Fig. 8e and f). However the surfaces still managed to stay hydrophobic by a decline in water CAs of around  $30$  and  $10^\circ$  after the same ultrasonication and annealing treatments, respectively.

The chemical stability testing of the hierarchical rough Al alloys coated with PFDCS and PFDCS verified the robustness of the coatings by retaining their strong repellency toward the three liquids studied. Strong covalent bonding through their polar tails onto the substrate could be the main reason behind the robustness of these coatings. It is also possible that PFDCS and PFDCS molecules might have achieved a more vertical orientation that can provide a close-packed configuration. A proper bonding and close packing of the molecules facilitate a self-assembled monolayer to be densely coated on the surface. In addition, the vertical orientation also allows the outward exposure of more  $-\text{CF}_3$  groups instead of  $-\text{CF}_2$  groups. The  $-\text{CF}_3$  group possess the lowest surface free energy of  $6$  mN/m compared to significantly higher surface free energy of  $16$  mN/m for the  $-\text{CF}_2$  group [9,10,35]. Meanwhile, the surfaces coated with PFDCS showed relatively better robustness, which could be an indication of a better adhesion and a consequently better close packing of the PFDCS molecules. On the other hand, deterioration of the PFOA coating on the hierarchical Al alloy surfaces is an indication of low adhesion of its polar tail to the substrate providing more horizontal orientation and subsequently higher  $-\text{CF}_2$  presence on the top surface.

Three dimensional (non-vertical) orientation of the fluorocarbon oligomers could cause less close packing of their molecules as well as the outward exposure of more  $-\text{CF}_2$  instead of  $-\text{CF}_3$ , lower  $-\text{CF}_3$ : $-\text{CF}_2$  ratios. For high surface tension liquids such as water, the variation in the exposure ratio of  $-\text{CF}_3$ : $-\text{CF}_2$  is less important. However, for low surface tension liquids such as oil, a higher exposure ratio of  $-\text{CF}_3$  is required to achieve superoleophobicity [30,31]. Therefore, we believe that a proper adhesion and close packing of the fluorocarbon oligomers could help in utilizing shorter fluorocarbon molecules to achieve superamphiphobicity. The usage of short fluorocarbon oligomers for developing SAP surfaces is also more environmentally friendly. In a recent work by Park et al. [36], it was shown that a flat oleophobic surface with low CAH can be obtained with an alkylsilane having an extremely short nonpolar fluorocarbon end of only one  $-\text{CF}_3$  group. Meanwhile, it should be noted that the superoleophobic surfaces and slippery oleophobic flat surfaces that have been obtained so far by utilizing short length fluorocarbon oligomers were not demonstrated so far to extend to self-assembly monolayer coatings of similar oligomers. In those studies, the substrate itself was made of a low surface energy fluorocarbon oligomer [11,36]. In this scenario, the close packing and subsequent exposure of more  $-\text{CF}_3$  groups is guaranteed. However, for a high surface energy metallic substrate, as in our case, an extreme close packing of the fluorocarbon oligomers' molecules with vertical orientation to prevent the penetration of low surface tension oils is more challenging. Therefore, more detailed studies

are needed to address the possibility of obtaining superoleophobic surfaces on high surface energy substrates by utilizing short length fluorocarbon oligomers.

#### 4. Conclusions

Three long-chain fluorocarbon oligomers of alkylsilanes and perfluorooctanoic acid were chemically vaporized onto hierarchically rough Al alloy surfaces that incorporate micro- and nano-scale features. These multi-scale rough Al alloy surfaces were produced by a simple and environmental friendly technique of one-directional mechanical sanding and treatment in boiling water. The effect of fluorocarbons' polar ends in facilitating a close packed self-assembled monolayer on the Al-alloy surfaces was investigated. In general, the alkylsilane oligomers showed higher liquid repellency toward both high and low surface tension liquids compared to the oligomer with acidic polar end. In addition, chemical stability tests revealed the enhanced robustness of the alkylsilane oligomers. A stronger bonding of the fluorocarbon oligomer by its polar end to the substrate may promote a more vertical orientation of its molecules and enhanced exposure of  $-\text{CF}_3$  groups instead of  $-\text{CF}_2$  groups. For developing surfaces with strong repellency toward oils, the surfaces need to be enriched with  $-\text{CF}_3$  groups. From the two alkylsilane oligomers studied, PFDCS showed a better chemical stability compared to PFDCS in spite of the longer overall carbon chain but similar fluorocarbon tail of the later one. Therefore, it can be concluded that there is a possibility of imparting SAP property to high surface energy solids utilizing a short fluorocarbon oligomer. This can be achieved by coating the re-entrant texture of the solid surface with a fluorocarbon oligomer which possess a polar end that can provide the high adhesion, close packing, and vertical orientation of its molecules. Consequently, this could facilitate a dominant ratio of  $-\text{CF}_3$  groups to be present at the liquid-solid interface instead of the higher surface energy  $-\text{CF}_2$  groups. Furthermore, the calculations of work of adhesion of the hierarchical surfaces showed that more realistic results can be obtained by considering both static and kinetic wetting measurements.

#### Acknowledgements

This work was supported in part by NASA (grant no.: NNX09AW22A) and NSF (grant no.: EPS-1003970). The authors thank UALR Center for Integrative Nanotechnology Sciences for helping with SEM measurements.

#### References

- [1] W. Barthlott, C. Neinhuis, Purity of the sacred lotus, or escape from contamination in biological surfaces, *Planta* 202 (1997) 1–8.
- [2] B. Bhushan, Y.C. Jung, K. Koch, Micro- nano- and hierarchical structures for superhydrophobicity, self-cleaning and low adhesion, *Philos. Trans. A Math. Phys. Eng. Sci.* 367 (2009) 1631–1672.
- [3] M. Nosonovsky, E. Bormashenko, Lotus effect: superhydrophobicity and self-cleaning, in: *Anonymous Functional Properties of Bio-Inspired Surfaces Characterization and Technological Applications*, World Scientific Publishing Co., Pte., Ltd., Singapore, Singapore, 2009, pp. 43–78.
- [4] X. Deng, L. Mammen, H. Butt, D. Vollmer, Candle soot as a template for a transparent robust superamphiphobic coating, *Science* 335 (2012) 67–70.
- [5] A. Tuteja, W. Choi, M. Ma, J.M. Mabry, S.A. Mazzella, G.C. Rutledge, G.H. McKinley, R.E. Cohen, Designing superoleophobic surfaces, *Science* 318 (2007) 1618–1622.
- [6] K. Liu, L. Jiang, Metallic surfaces with special wettability, *Nanoscale* 3 (2011) 825.
- [7] K. Liu, Y. Tian, L. Jiang, Bio-inspired superoleophobic and smart materials: design, fabrication, and application, *Prog. Mater. Sci.* 58 (2013) 503–564.
- [8] S. Shibuchi, T. Yamamoto, T. Onda, K. Tsujii, Super water- and oil-repellent surfaces resulting from fractal structure, *J. Colloid Interface Sci.* 208 (1998) 287.
- [9] J. Tsiabouklis, T.G. Nevell, Ultra-low surface energy polymers: the molecular design requirements, *Adv. Mater.* 15 (2003) 647–650.

- [10] T. Nishino, M. Meguro, K. Nakamae, M. Matsushita, Y. Ueda, Lowest surface free energy based on CF<sub>3</sub> alignment, *Langmuir* 15 (1999) 4321–4323.
- [11] H. Bellanger, T. Darmanin, F. Guittard, Surface structuration (micro and/or nano) governed by the fluorinated tail length toward superoleophobic surfaces, *Langmuir* 28 (2013) 186–192.
- [12] M. Liu, S. Wang, Z. Wei, Y. Song, L. Jiang, Bioinspired design of a superoleophobic and low adhesive water/solid interface, *Adv. Mater.* 21 (2009) 665–669.
- [13] H. Meng, S. Wang, J. Xi, Z. Tang, L. Jiang, Facile means of preparing superamphiphobic surfaces on common engineering metals, *J. Phys. Chem. C* 112 (2008) 11454–11458.
- [14] S. Peckook, B. Pokroy, Bioinspired hierarchical superhydrophobic structures formed by *n*-paraffin waxes of varying chain lengths, *Soft Mater.* 9 (2013) 5710–5715.
- [15] K. Tsujii, T. Yamamoto, T. Onda, S. Shibuichi, Super oil-repellent surfaces, *Angew. Chem. Int. Ed. Engl.* 36 (1997) 1011–1012.
- [16] Z.S. Saifaldeen, K.R. Khedir, M.F. Cansizoglu, T. Demirkan, T. Karabacak, Superamphiphobic aluminum alloy surfaces with micro and nanoscale roughness produced by a simple and environmentally friendly technique, *J. Mater. Sci.* 49 (2014) 1839–1853.
- [17] H. Zhao, K. Park, K. Law, Effect of surface texturing on superoleophobicity, contact angle hysteresis, and robustness, *Langmuir* 28 (2012) 14925–14934.
- [18] C.-T. Hsieh, F.-L. Wu, W.-Y. Chen, Superhydrophobicity and superoleophobicity from hierarchical silica sphere stacking layers, *Mater. Chem. Phys.* 121 (2010) 14–21.
- [19] Y. Guo, Q. Wang, T. Wang, Facile fabrication of superhydrophobic surface with micro/nanoscale binary structures on aluminum substrate, *Appl. Surf. Sci.* 257 (2011) 5831–5836.
- [20] K.R. Khedir, Z.S. Saifaldeen, T.M. Demirkan, A.A. Al-Hilo, M.P. Brozak, T. Karabacak, Robust superamphiphobic nanoscale copper sheet surfaces produced by a simple and environmentally friendly technique, *Adv. Eng. Mater.* 17 (2014) 982–989.
- [21] Y. Sheen, Y. Huang, C. Liao, H. Chou, F. Chang, New approach to fabricate an extremely super-amphiphobic surface based on fluorinated silica nanoparticles, *J. Polym. Sci. Part B* 46 (2008) 1984–1990.
- [22] C.-T. Hsieh, F.-L. Wu, W.-Y. Chen, Super water- and oil-repellencies from silica-based nanocoatings, *Surf. Coat. Technol.* 203 (2009) 3377–3384.
- [23] H.F. Hoefnagels, D. Wu, G.D. With, W. Ming, Biomimetic superhydrophobic and highly oleophobic cotton textiles, *Langmuir* 23 (2007) 13158–13163.
- [24] H. Zhao, K. Law, V. Sambhy, Fabrication, surface properties, and origin of superoleophobicity for a model textured surface, *Langmuir* 27 (2011) 5927–5935.
- [25] T. Karabacak, Thin-film growth dynamics with shadowing and re-emission effects, *J. Nanophoton.* 5 (2011) 052501.
- [26] Xiaoyan Song, Jin Zhai, Yilin Wang, Lei Jiang, Fabrication of superhydrophobic surfaces by self-assembly and their water-adhesion properties, *J. Phys. Chem. B* 109 (2005) 4048–4052.
- [27] K.R. Khedir, G.K. Kannarpady, H. Ishihara, J. Woo, S. Trigwell, C. Ryerson, A.S. Biris, Advanced studies of water evaporation kinetics over teflon-coated tungsten nanorod surfaces with variable hydrophobicity and morphology, *J. Phys. Chem. C* 115 (2011) 13804–13812.
- [28] C. Hsieh, F. Wu, W. Chen, Contact angle hysteresis and work of adhesion of oil droplets on nanosphere stacking layers, *J. Phys. Chem. C* 113 (2009) 13683–13688.
- [29] M. Miwa, A. Nakajima, A. Fujishima, K. Hashimoto, T. Watanabe, Effects of the surface roughness on sliding angles of water droplets on superhydrophobic surfaces, *Langmuir* 16 (2000) 5754–5760.
- [30] A. Hozumi, T.J. McCarthy, Ultralyophobic oxidized aluminum surfaces exhibiting negligible contact angle hysteresis, *Langmuir* 26 (2010) 2567–2573.
- [31] A. Hozumi, B. Kim, T.J. McCarthy, Hydrophobicity of perfluoroalkyl isocyanate monolayers on oxidized aluminum surfaces, *Langmuir* 25 (2009) 6834–6840.
- [32] Y. Xiu, L. Zhu, D.W. Hess, C.P. Wong, Relationship between work of adhesion and contact angle hysteresis on superhydrophobic surfaces, *J. Phys. Chem. C* 112 (2008) 11403–11407.
- [33] C. Lv, C. Yang, P. Hao, F. He, Q. Zheng, Sliding of water droplets on microstructured hydrophobic surfaces, *Langmuir* 26 (2010) 8704–8708.
- [34] E. Bormashenko, Y. Bormashenko, Wetting of composite surfaces: when and why is the area far from the triple line important? *J. Phys. Chem. C* 117 (2013) 19552–19557.
- [35] C.J. Faulkner, R.E. Fischer, G.K. Jennings, Surface-initiated polymerization of 5-(perfluoro-*n*-alkyl)norbornenes from gold substrates, *Macromolecules* 43 (2010) 1203–1209.
- [36] J. Park, C. Urata, B. Mashed, D.F. Cheng, A. Hozumi, Long perfluoroalkyl chains are not required for dynamically oleophobic surfaces, *Green Chem.* 15 (2013) 100–104.